Optimization of Ti/IrO_2-Sb_2O_3 anode material coating composition for high electrochemically active area using response surface method

Pavithra Bhakthi Jayathilaka
National Institute of Fundamental Studies
Athula Bandara
Department of Chemistry, University of Peradeniya
Nadeeshani Nanayakkara
Department of Civil Engineering, University of Peradeniya
Nalaka Deepal Subasinghe (✉ deepal.su@nifs.ac.lk)
National Institute of Fundamental Studies

Research Article

Keywords: Electrochemical oxidation, Ti/IrO2-Sb2O3 anode material, Optimization, Response surface methodology, Water treatment

Posted Date: April 27th, 2023

DOI: https://doi.org/10.21203/rs.3.rs-2854668/v1

Abstract

Anode material plays big role in electrochemical oxidation process of water treatment. Since its coating composition can affect the degradation path way, the reaction mechanism and the efficiency of electrochemical oxidation process, it is important to identify the optimum conditions of a given material composition of a high electrochemical active area. In this work, central composite design with response surface method was implemented to optimize Ir and Sb contents of Ti/IrO_2-Sb_2O_3 anode. In order to do that, response factors (i.e. anodic charge and open circuit potential value), which are related to electrochemically active area of the anode were monitored. They were expressed in second-order functions of two factors such as Ir and Sb concentrations. Since these factors showed significant impact on anodic charge and open circuit potential values of the anode, statistical analysis was done in order to gain the understanding of them. ANOVA table results, R^2 and R_{adj} values, *lack of fit* test and *p* values indicated that the models represent experimental data well. 3-D response surface and 2-D contour plots visualized the effects. Overall analysis of results found that 0.3625 mC anodic charge value and -0.0869 mV open circuit value can be obtained by optimum material conditions of 0.08 g/L and 0.92 g/L Ir and Sb concentrations respectively.

INTRODUCTION

Water bodies in human habitat areas are often polluted, especially with organics, mainly due to addition of industrial effluents (Cartaxo et al., 2012). Since these water bodies are directly or indirectly connected with the major sources of drinking water supplies, their quality management and treatment are important. In order to enhance the usefulness of water environment, developing techniques to treat water polluted with organic chemicals are essential. Among different water treatment techniques, applications on electrochemical oxidation are more attractive (Li et al., 2005; Cui et al., 2009; Jayathilake et al. 2014). In the electrochemical oxidation process the anode material plays a major role (Zheng et al., 2011; Jayathilake et al. 2015; 2017).

Therefore, development of novel anode materials has received more attention recently. A reasonable number of attempts were made to develop novel anode materials such as boron-doped diamond (Canizares et al., 2005), Ti/Pt–Ir, Ti/PbO_2, $Ti/PdO–Co_3O_4$ and $Ti/RhO_x–TiO_2$ (Szpyrkowicz et al., 2005), graphite (Ogutveren et al., 1999), graphite/steel (Abou-Taleb et al., 2021) Pb/PbO_2 (Nava et al., 2008), Ti/SnO_2-Sb_2O_5/PbO_2 (Xue et al., 2011), $Ti/RuO_2–TiO_2$ (Feng et al., 2003; Radjenovic et al., 2011) and Ti/SnO_2-Sb (Fockedey and Llierde, 2002). Moreover, there are many studies on anode system optimum operating conditions such as pH, temperature, flow rate, current density, initial pollutant concentration and supporting electrolyte concentration for efficient electrochemical oxidation process (Wu et al., 2007).

However, number of studies on anode material composition optimization are lacking and falling short of the anode development studies. Composition of the coating of the anode has a significant effect on degradation path way, reaction mechanism and the efficiency of electrochemical oxidation process.

Therefore, it is important to determine the optimum material composition for a given anode, to maximize the electrochemically active area. When the electrochemically active area of anode material is enhanced, efficiency of electrochemical oxidation of pollutants increases. Further, optimization of the anode material has a direct effect on the cost of production and operation. Therefore, the aim of this study is to develop novel Ti/ IrO_2-Sb_2O_3 anode material with optimum Ir and Sb composition for the highest electrochemical active area.

Hence, this study is focused on development and optimization of Ti/ IrO_2-Sb_2O_3 anode material with using *response surface* method. Response surface method (RMS) is one of the popular statistical methods used in similar applications. It has been used to study and optimize complex systems with factors and response variables (E.g. Yong et al. 2009; Körbahti and Demirbüken, 2017). Since electrochemically active area can be monitored by anodic charge and open circuit potential (OCP) values of the anode material, anodic charge and the OCP values were taken as the response variables. Ir and Sb concentrations were taken as the two independent factors for the development of optimization models. In this study the models were validated through statistical analysis and in order to gain the understanding of them ANOVA table results, R^2 and R_{adj} values, *lack of fit* test results and p values were monitored. Predicted values by the models were proved through experimental studies on anodic charge and open circuit potential (OCP) of the anode. 3-D response surface and 2-D contour plots were used to visualize the optimum conditions. Finally, the identified optimum conditions were verified experimentally.

MATERIALS & METHOD

Materials

All the chemicals used were analytical grade, including Sb standard solution (Fisher Scientifics), ethanol (99%, AR, Fisher Scientifics), isopropanol, H_2SO_4 (98%, Fisher Scientifics), Na_2SO_4 anhydrous (AR, 99%, SDFCL), $H_2C_2O_4.2H_2O$ (99%, LOBAL Chemie), HCl (37%, BDH), $IrCl_3.3H_2O$ (Ir – 53–56%, ACRDS Organics). Deionized (DI) water was used to prepare aqueous solutions.

Ti/IrO_2-Sb_2O_3 anode system

Fifteen Ti/IrO_2-Sb_2O_3 anodes with geometrical area of ~ 1 cm^2 were prepared with different anode material compositions. Prior to coating the anode, Ti substrate material was mechanically treated by a sand paper with grit of 120 and then chemically pre-treated with 5% (w/w) oxalic acid solution and 37% (w/w) HCl. The mechanical treatment helped to enhance the adhesive properties of anodes while chemical treatment removes contaminants and oxide layers on the surface. Then anodes were washed with DI water and dried at 100°C as mentioned in Feng and Johnson (1991). Next, coating solutions were applied until the final coating load of 1 mg/cm^2 is achieved. These coating solutions were prepared by mixing $IrCl_3.3H_2O$ in ethanol and Sb (1000 ppm) standard solution in isopropanol (Min et al., 2007). Subsequently, the solvents on anodes were evaporated by air drying at 80°C. Then all anodes were calcinated at 450°C for 10 min and post backed at 500°C in muffle furnace (OT-HTMF-05, Optics technology, Delhi India) for 1 h (Min et al., 2007).

Response surface methodology

The effects of variables and their responses on Ti/IrO_2-Sb_2O_3 anodes' electrochemical oxidation performance were studied by using a tool (i.e. design of experiments (DOE)) in Minitab® 16 software. In order to determine the influences of specified parameters and optimum conditions of Ti/IrO_2-Sb_2O_3 anode, response surface methodology (RSM) was used. It was one of the DOEs widely applied in such studies. In RMS, sequential experimental studies were designed through second order designs called central composite design (CCD). It was well suited for the process optimization due to reasonable information with less number of design points (Zhu et al., 2010, Wei et al., 2011). According to the design, 13 experiments were suggested. Ir (C_{Ir}) and Sb (C_{Sb}) concentrations were selected as independent variables and their experimental ranges were set as in Table 1.

Table 1: Experimental range and levels of independent factors for anode performance

Independent factors	Factor	Range and levels	
	x_i	**-1**	**1**
Ir concentration (g/L)	x_1	0.1	0.15
Sb concentration (g/L)	x_2	0.2	0.8

Therefore, CCD studies were conducted to find out their significant effects on Ti/IrO_2-Sb_2O_3 anode performance. The response variables were anodic charge and open circuit potential (OCP) voltage of the anode. The relationship between factors and the responses was investigated statistically by using a multiple regression model as follows,

$$Y = f(x) = \beta_0 + \sum_{i=1}^{k} \beta_i x_i + \sum_{i=1}^{k} \sum_{j=i+1}^{k} \beta_{ij} x_i x_j + \sum_{i=1}^{k} \beta_{ii} x_i^2 \qquad (1)$$

Where Y is the predicted response value of anodic charge or open circuit potential (OCP) voltage, k is number of independent variables. In this study there are 2 independent variables namely, Ir concentration and Sb concentration. β_0 is the constant coefficient and β_i is linear coefficient while $\beta_{ij}$and β_{ii} are interaction and quadratic term of the equation respectively.

Analytical method

Response variables; OCP and anodic charge were measured through Autolab potentiostat-galvanostat (Autolab PGSTAT128N). In order to calculate anodic charge values cyclic voltammetry graphs were obtained. The electrode under study was used as the working electrode (WE). While Ti was used as cathode, Ag/AgCl electrode was used as the reference electrode (RE). Scan rate was set to 0.05 V/s. Range of voltage scan was from − 2.5 V to 2.5 V. Sulfuric acid (0.5 M) 25 ml solution was used as the electrolyte.

In open circuit potential measurements, Ti cathode and Ag/AgCl reference electrode were used. Under zero current conditions (i.e. Chronopotentiometry method), the OCP was monitored until the value was stabilized. Physical surface area of the electrodes was maintained at 1 cm^2 in all the cases.

RESULTS AND DISCUSSION

Fitted model development and validation for Ti/IrO_2-Sb_2O_3 anode system

According to CCD, thirteen experimental conditions of two factors were tested and response results were obtained as in Table 2. These results were used in model development by the least square method. The two responses (i.e. anodic charge and OCP) and two factors (i.e. Ir and Sb concentration) were correlated base on the second-order polynomial function (Eq. 1). The experimental results were used to develop quadratic regression models as in the equations 2 and 3 below.

$$Y_1 = 1.3269 - 19.4463x_1 + 0.6692x_2 + 77.6207x_1^2 - 0.1931x_2^2 + -3.6016x_1x_2 \,(2)$$

(R^2 = 94.5%, R^2adj = 90.7%)

$$Y_2 = 0.791 - 29.491x_1 + 3.585x_2 + 124.6x_1^2 - 0.774x_2^2 + -20.667x_1x_2 \,(3)$$

(R^2 = 90.2%, R^2adj = 83.1%)

Where x_1 *and* x_2 denote Ir, Sb concentrations and Y_1 and Y_2 denote anodic charge value and OCP value respectively. In the equations 2 and 3, the coefficients of x_1 and x_2 (i.e. coefficients with one factor) represent the effect of that particular factor. For an example, the coefficient values 19.4463x_1 in Eq. 2 shows the Ir concentration effect on anodic charge (i.e. Y_1).

Moreover, coefficients with two factors (e.g.$3.6016x_1x_2$) and coefficients with second-order (i.e. $3.6016x_1x_2$) represent both interaction between two factors effect on response and quadratic effect of each factor on response, respectively. The synergetic effect is implied by the negative sign and the antagonistic effect is indicated by the positive sigh. Therefore, according to Eqs. 2 and 3 Ir concentration had antagonistic individual effect on both anodic charge and OCP values while Sb concentration gave synergetic effect on them individually

In detail these two models showed high coefficient of determination values (i.e. R^2). They were 94.5% and 90.2% for anodic charge and OCP values respectively. Therefore, there was better agreement between experimental and predicted results. Since R^2 is close to 1, it indicates that above two models explained the predictions satisfactorily. Hence, outcome results implied that RMS was suitable for anode material optimization.

Table 2: CCD and the results obtained

	Experimental design		Results			
Run	Ir Concentration (x_1)	Sb Concentration (x_2)	(Y_1), Anodic charge (mC)		(Y_2),OCP (mV)	
			Experimental	Predicted	Experimental	Predicted
1	0.100	0.800	0.262523	0.282125	-0.12	-0.19
2	0.125	0.500	0.164260	0.170161	-0.62	-0.64
3	0.125	0.500	0.164390	0.170161	-0.60	-0.64
4	0.125	0.924	0.150574	0.146428	-0.71	-0.68
5	0.150	0.200	0.184623	0.174489	-0.62	-0.76
6	0.125	0.500	0.166375	0.170161	-0.66	-0.64
7	0.090	0.500	0.358420	0.329714	-0.17	-0.18
8	0.150	0.800	0.146750	0.136005	-0.85	-0.94
9	0.125	0.500	0.169730	0.170161	-0.64	-0.64
10	0.160	0.500	0.185252	0.200779	-0.93	-0.79
11	0.125	0.500	0.185837	0.170161	-0.69	-0.64
12	0.125	0.076	0.129532	0.124465	-0.98	-0.87
13	0.100	0.200	0.192348	0.212561	-0.60	-0.64

In order to ensure that the fitted model is adequately compatible with the real system, validating the model is required. Therefore, above two models on anodic charge and OCP were tested to prevent them from misleading optimization results. The model validation was done with both graphical and experimentally. In graphically studied, the nature of residuals by using both plots on residuals vs. fitted values (Fig. 1) and residuals vs. observed values (Fig. 2). Since residuals means the difference between fitted *Y* value and observed *Y* value, those graphs gave detail picture of residuals nature.

Moreover, the intention of plotting residuals vs. fitted values was to test the functional part of the model while the graph on residuals vs. observed values was used in identifying drifts of the process of the model. According to the results both plots show no significant difference in values. They were randomly distributed and there was no obvious pattern. Therefore, models were capable to provide adequate approximations to the real system conditions. In addition, residuals were tested with normal probability plots. As in Fig. 3 normal probability plots of residuals data lay on theoretical straight line and were not significant deviations. According to the theory if there is departure from straight line, it means residuals are not in normal distribution. Since Fig. 3 also was satisfied the requirements, the models were success in graphical validation.

Then numerical model validation was conducted with ANOVA analysis. The resulted probabilities of p values in the regression were 0.002 and 0.000 for anodic charge and OCP models respectively. Due to very low p > F values in ANOVA table results, those models were highly significant. Moreover the lack of fit test s' p values were compared. Since this lack of fit explains the variation of data around the fitted model, when it gives larger p values the model does not fit with data well. Therefore in the case of lack of fit does not fit the model, it will be significant. In Table 3 ANOVA results observed that there was large p values of 0.010 and 0.035 for lack of fit of anodic charge and OCP models. Hence, the models explained the data well.

Table 3: ANOVA results for 2 responses (Anodic charge and OCP)

	DF	Sum of square	Mean square	F-value	p > F
Anodic charge					
Regression	5	0.596225	0.119245	12.83	0.002
Total error	7	0.065052	0.009293		
Lack of fit	3	0.060172	0.020057	16.44	0.010
Pure error	4	0.004880	0.001220		
OCP					
Regression	5	0.040714	0.008143	24.28	0.000
Total error	7	0.002347	0.000335		
Lack of fit	3	0.002019	0.000673	8.20	0.035
Pure error	4	0.000328	0.000082		

Optimization analysis

The optimized conditions were identified through three dimensional surface plots (Fig. 4) and two dimensional contour plots (Fig. 5). Since these surface-counter plots are the graphical representation of regression models, they were developed as a function of Ir and Sb concentrations. Therefore, these results help to visualize relationship between response and experimental factor levels. As seen in Fig. 4 (a) anodic charge was increased when Ir concentration was lower and Sb concentration was high. The catalytic activity of the Sb enhances the electrochemically active area. This caused to increment in anodic charge values. Similar pattern was observed for the OCP variations (Fig. 4 (b)). With increasing Sb concentrations and decreasing Ir concentrations OCP values were high. Since, higher the electrode stability, it gives high OCP values. Therefore, this type of Ir and Sb combination caused improvement of electrodes' stability. Moreover both surface and counter plots showed that at Ir concentration higher than 0.1 g/L, both anodic charge and OCP values began to decrease.

Since these anodic charge and OCP are two individual independent responses, their optimization conditions are different. In order to verify exact optimized levels of these factors, response surface-contour analyses were conducted based on Eqs. 2 and 3. According to the Eq. 4 optimum conditions were identified where the derivation is zero.

$$\frac{\partial Y}{\partial X_1} = \frac{\partial Y}{\partial X_2} = 0$$

4

It was 0.08964 g/L and 0.92426 g/L Ir and Sb concentrations respectively. At these optimized conditions the model predicted Ti/IrO_2-Sb_2O_3 anodes' optimum anodic charge as 0.36251 mC and OCP as -0.08696 mV. More over optimized conditions for simultaneous responses can be visualized by overlain counter plot of anodic charge and OCP (Fig. 6).

Moreover, in order to confirm the results obtained from the model and experiments, two additional experiments were conducted on optimized conditions. Results of those experiments are shown in Table 4. Experimental and predicted model optimization condition values are in very close agreement. .

Table 4: Confirmation of experiment results of optimized conditions

	Coating material composition (g/L)		**Responses**	
	Ir concentration	**Sb concentration**	**Anodic charge (mC)**	**OCP (mV)**
Experimental values	0.08964	0.924	0.3763	-0.08581
Predicted values	0.08964	0.924	0.36251	-0.08696
Error (%)			3.08	1.32

CONCLUSIONS

Since anode material composition has great impact on electrochemical oxidation performance of phenol, this work was conducted to identify the optimum conditions of coating materials by using RSM model. Both anodic charge and OCP values were monitored as responses. RSM model was performed with 3-D response surface and 2-D contour plots. Based on the results and analysis following conclusions were drawn.

1. According to regression models, Ir and Sb concentrations have significant effect on anodic charge value of Ti/IrO_2-Sb_2O_3 anodes and its OCP value. Since both anodic charge and OCP values are related to anodes electrochemical oxidation performance, performance can be enhanced by varying the concentrations of Ir and Sb.
2. Maximum anodic charge and OCP were resulted at the Ir and Sb concentrations of 0.08964 g/L and 0.924 g/L respectively. Optimum anodic charge was 0.36251 mC and the corresponding OCP value was 0.08696 mV. Subsequently this was confirmed by the overlain contour plot.
3. Finally, the experimental results were found to be in good agreement with the predicted model, proving that the use of RSM and CCD tools are successful in anode material optimization.

References

1. Abou-Taleb, E.M. ,Hellal, M.S., Kamal, K.H. (2021) Electro-oxidation of phenol in petroleum wastewater using a novel pilot-scale electrochemical cell with graphite and stainless-steel electrodes. Water and Environmental Journal, **35,** 259-268.
2. Canizares, P., Lobato, J., Paz, R., Rodrigo, M.A., Saez, C., (2005). Electrochemical oxidation of phenolic wastes with boron-doped diamond anodes. Water Research, 39(12), 2687- 2703.
3. Cartaxo, M.A.M., Ablad, K., Douch, J., Berghoute, Y., Hamdani, M., Mendonca, M.H., Nogueira, J.M.A., Pereira, M.I.S., (2012). Phenol electro oxidation on Fe-Co_3O_4 thin film electrodes in alkaline medium. Chemosphere, 86(4), 341-347.
4. Cui, Y., Li, X., Chen, G., (2009). Electrochemical degradation of bisphenol A on different anodes. Water Research, 43(7), 1968-1976.
5. Feng, C., Sugiura, N., Shimada, S., Maekawa, T., (2003). Development of a high performance electrochemical wastewater treatment system. Journal of Hazardous Materials, 103(1-2), 65–78.
6. Feng, J., & Johnson, D.C. (1991). Electrocatalysis of Anodic Oxygen-Transfer Reactions: Titanium Substrates for Pure and Doped Lead Dioxide Films. Journal of the Electrochemical Society, 138(11), 3328-3337.
7. Feng, Y.J., & Li, X.Y. (2003). Electro-catalytic oxidation of phenol on several metal-oxide electrodes in aqueous solution. Water Research, 37(10), 2399-2407.
8. Fockedey, E., & Lierde, A.V. (2002). Coupling of anodic and cathodic reactions for phenol electro-oxidation using three-dimensional electrodes. Water Research, 36(16), 4169-4175.
9. Jayathilaka, P.B., Hapuhinna, K.U.K, Bandara, A., Nanayakkara, A. and Subasinghe, N.D. (2017) Phenol contaminated water treatment on several modified dimensionally stable anodes. Water

Environment Research. 89 (8), 687-693.

10. Jayathilaka, P.B., Pathiraja, G.C., Bandara, A., Subasinghe, N.D. and Nanayakkara, N. (2015). Electrochemical oxidation of phenol on Steel/IrO2-Sb2O3 electrodes: a mechanisms study, Canadian Journal of chemistry. 93, 536-541.
11. Jayathilaka, P.B., Pathiraja, G.C., Bandara, A., Subasinghe, N.D., and Nanayakkara, N. (2014) Theoretical study of phenol and hydroxyl radical reaction mechanism in aqueous medium by DFT/ B3LYP/ 6-31+G (d, p)/ CPCM model. Canadian Journal of Chemistry. 92(9), 809-813.
12. Körbahti BK and Demirbüken P (2017) Electrochemical Oxidation of Resorcinol in Aqueous Medium Using Boron-Doped Diamond Anode: Reaction Kinetics and Process Optimization with Response Surface Methodology. Front. Chem. 5:75. doi: 10.3389/fchem.2017.00075
13. Li, X., Cui, Y., Feng, Y., Xie, Z., Gu, J., (2005). Reaction pathways and mechanisms of the electrochemical degradation of phenol on different electrodes. Water Research, 39(10), 1972–1981.
14. Min, T., Linda, B., Aicheng, C., (2007). Kinetics of the electrochemical oxidation of 2-nitrophenol and 4-nitrophenol studied by in situ UV spectroscopy and chemometrics. Electrochimica Acta, 52(23), 6517–6524.
15. Nava, J.L., Quiroz, M.A., Martínez-Huitle, C.A., (2008). Electrochemical Treatment of Synthetic Wastewaters Containing Alphazurine A Dye: Role of Electrode Material in the Colour and COD Removal. Journal of the Mexican Chemical Society, 52(4), 249-255.
16. Ogutveren, U.B., Toru, E., Koparal, S., (1999). Removal of cyanide by anodic oxidation for wastewater treatment. Water Research, 33(8), 1851-1856.
17. Radjenovic, J., Bagastyo, A., Rozendal, R.A., Mu, Y., Keller, J., Rabaey, K., (2011). Electrochemical oxidation of trace organic contaminants in reverse osmosis concentrate using RuO_2/IrO_2-coated titanium anodes. Water Research, 45(4), 1579 -1586.
18. Szpyrkowicz, L., Santosh N.K., Neti, R.N., Satyanarayan, S., (2005). Influence of anode material on electrochemical oxidation for the treatment of tannery wastewater. Water Research, 39(8), 1601-1613.
19. Wei, J., Zhu, X., Ni, J., Electrochemical oxidation of phenol at boron-doped diamond electrode in pulse current mode. 2011. Electrochimica Acta. 56, 5310-5315.
20. Wu, D., Liu, M., Dong, D., Zhou, X., (2007). Effects of some factors during electrochemical degradation of phenol by hydroxyl radicals. Microchemical Journal, 85(2), 250-256.
21. Wu, D., Liu, M., Dong, D., Zhou, X., (2007). Effects of some factors during electrochemical degradation of phenol by hydroxyl radicals. Microchemical Journal, 85(2), 250-256.
22. Xue, B., Zhang, Y., Wang, J.Y., (2011). Electrochemical oxidation of Bisphenol A on Ti/SnO_2-Sb_2O_5/PbO_2 anode for waste water treatment. Procedia Environmental Sciences. 10(A), 647-652.
23. Yang, D.C., Jang, I.S., Jang, M.H., Park, C-N., Park, C.J. (2009) Optimization of additive compositions for anode in Ni-MH secondary battery using the response surface method. Met. Mater. Int. 15, 421–425.

24. Zheng, Y., Su, W., Chen, S., Wu, X., Chen, X., (2011). Ti/SnO_2-Sb_2O_5- RuO_2/α-PbO_2/β-PbO_2 electrodes for pollutants degradation. Chemical Engineering Journal, 174(1), 304-309.
25. Zhu, X., Ni, J., Wei, J., Xing, X., Li, H., Jiang, Y..(2010) Scale-up of BDD anode system for electrochemical oxidation of phenol simulated wastewater in continuous mode. Journal of Hazardous Materials. 184, 493-498.

Figures

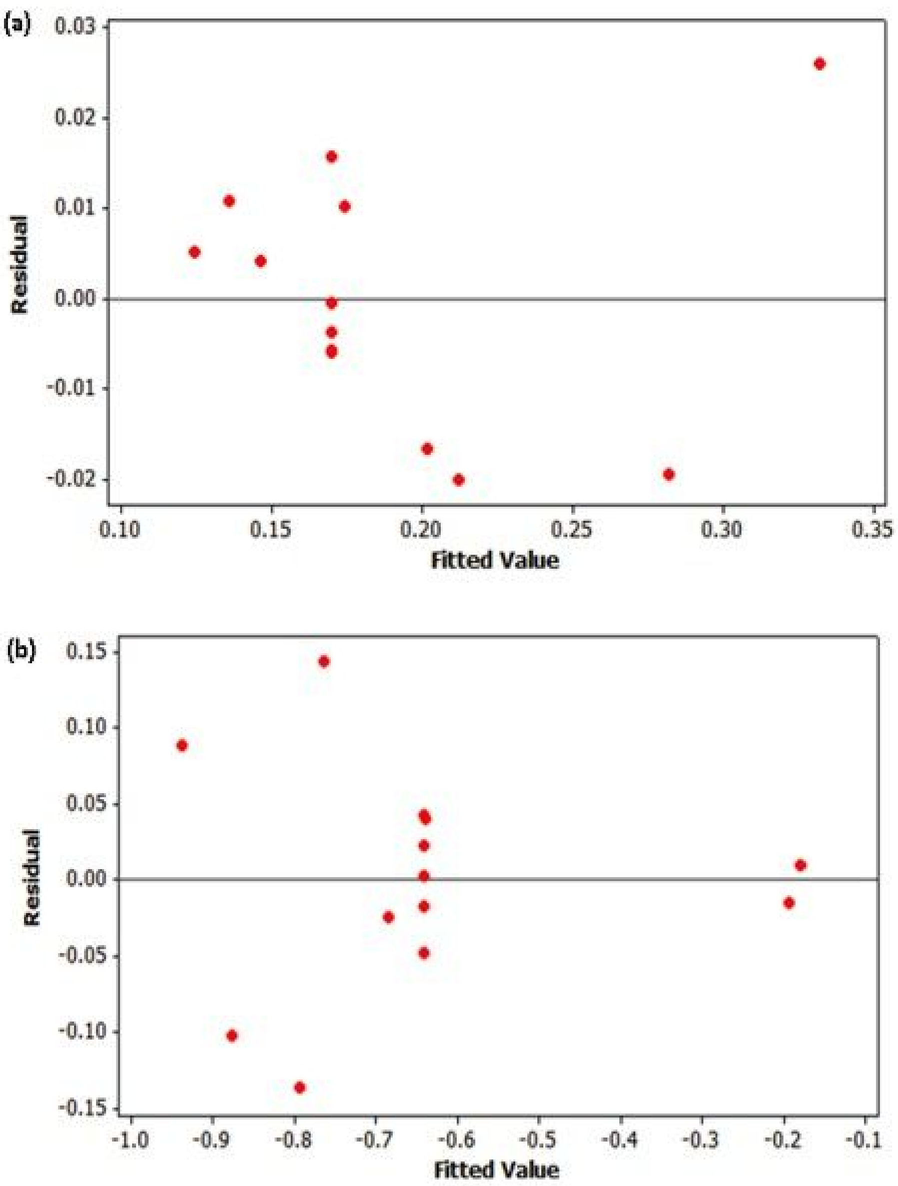

Figure 1

Residuals vs. fitted values for (a) anodic charge and (b) OCP

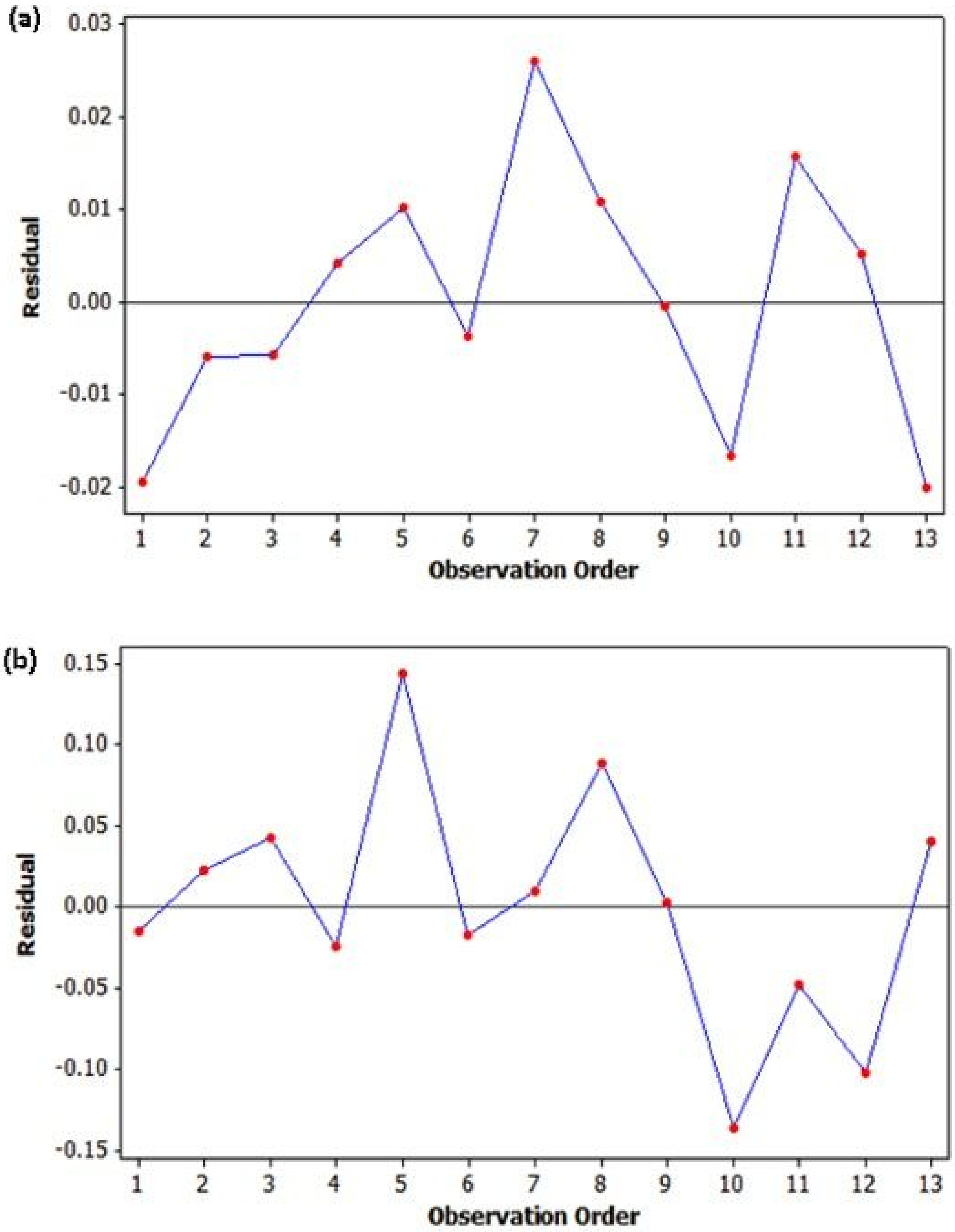

Figure 2

Residuals vs. observation orders of data (a) anodic charge and (b) OCP

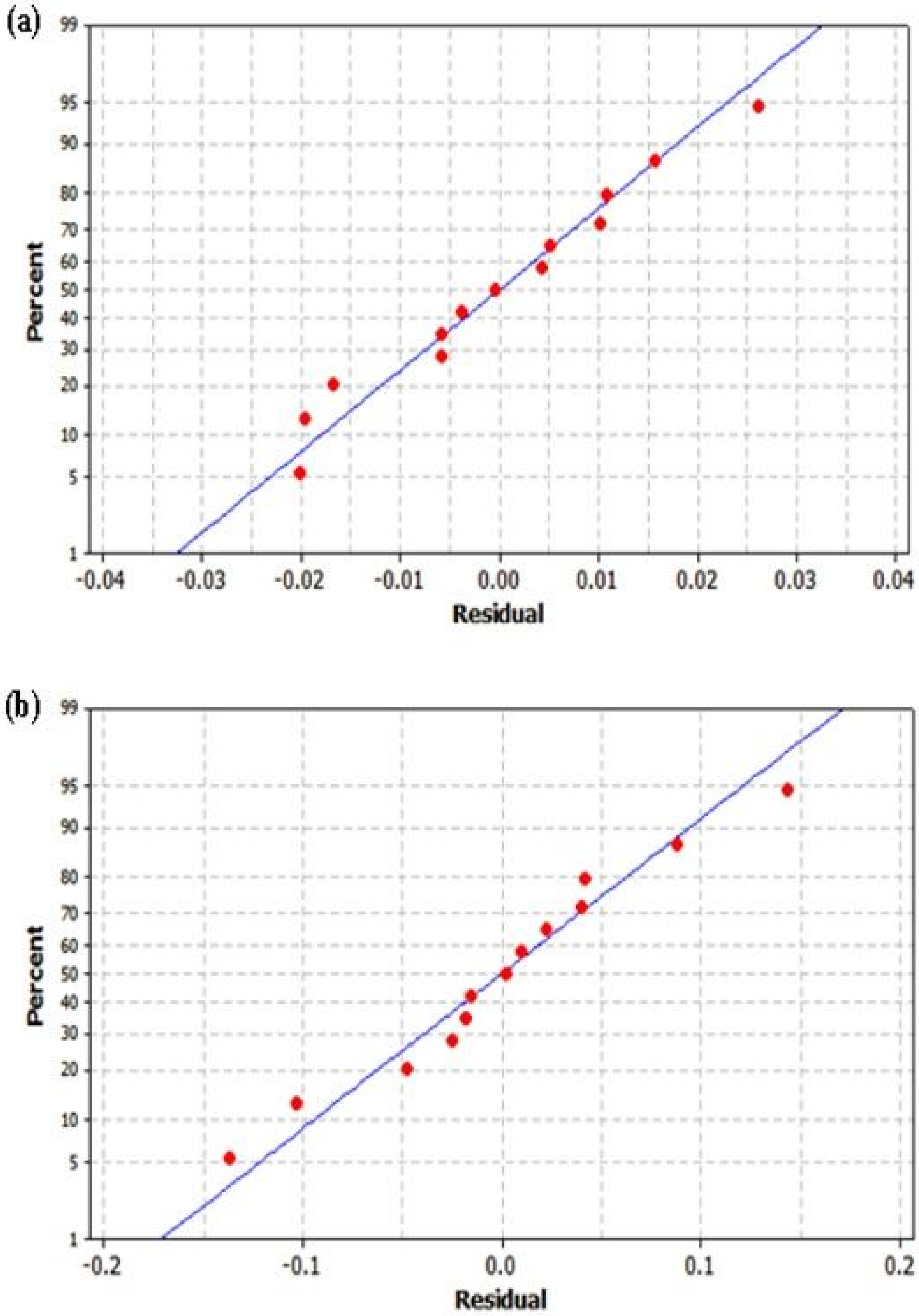

Figure 3

Normal probability plots for (a) anodic charge and (b) OCP

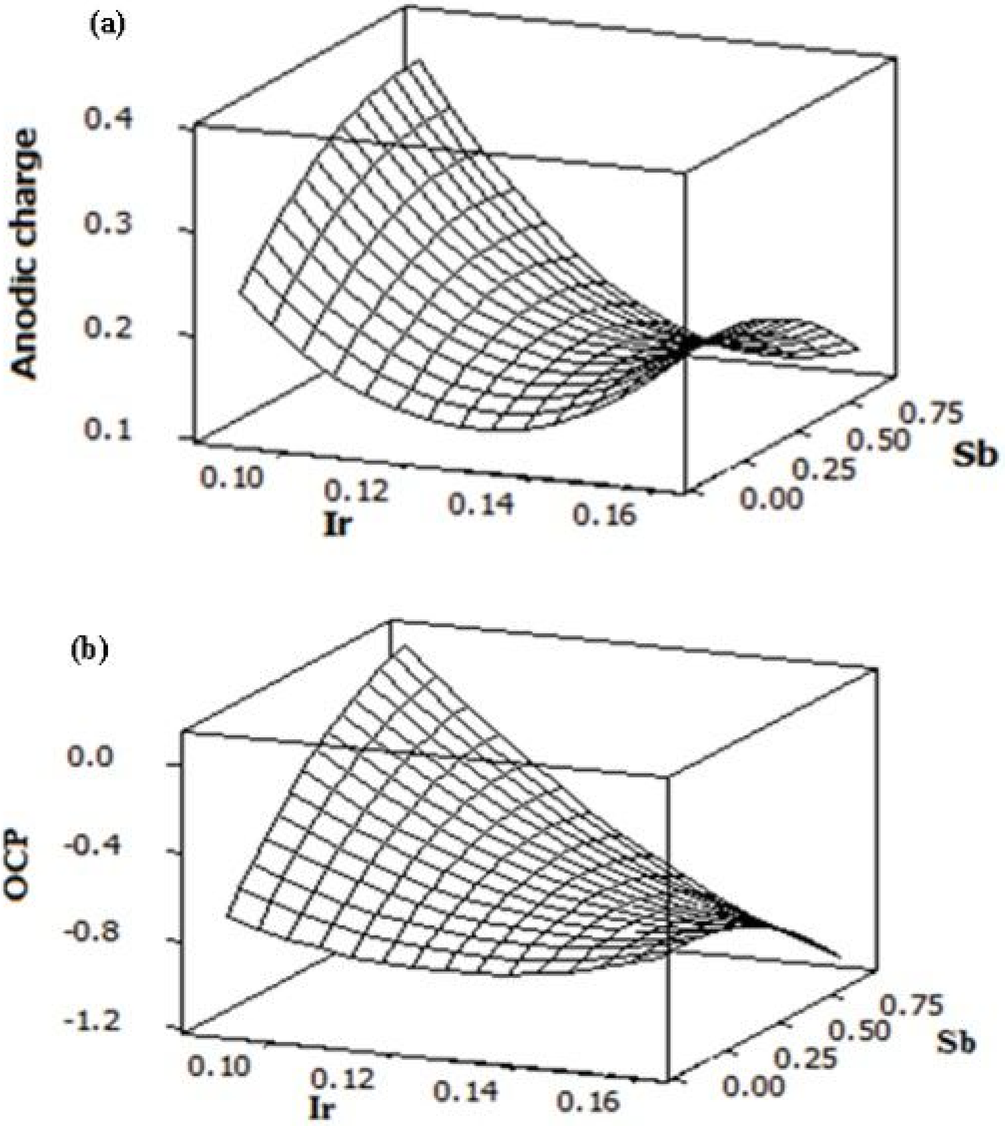

Figure 4

Three dimensional surface plots for (a) anodic charge and (b) OCP

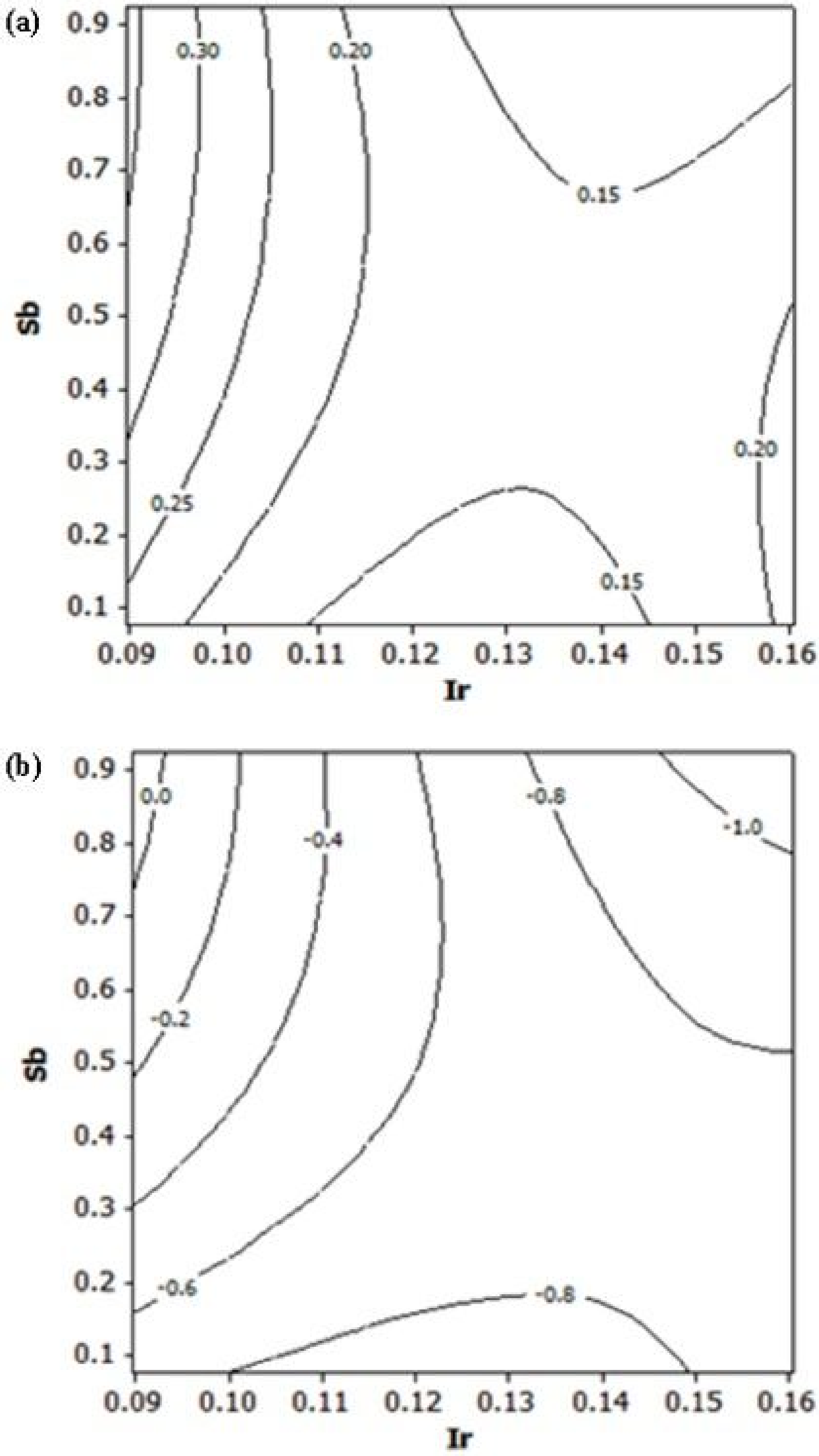

Figure 5

Two dimensional contour plots for (a) anodic charge and (b) OCP

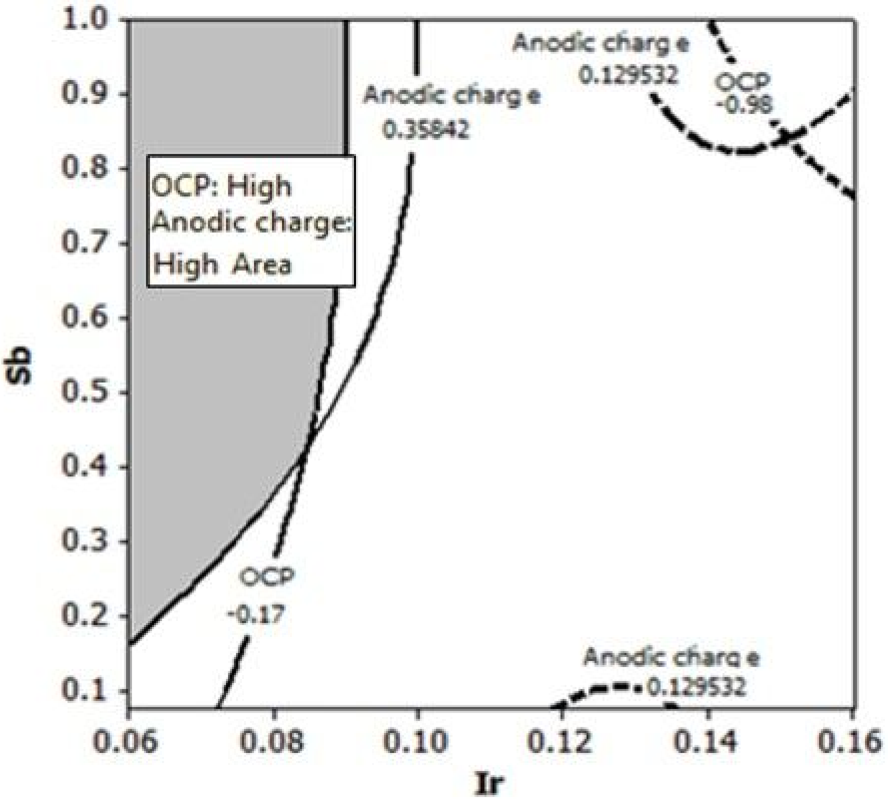

Figure 6

Overlain contour plot of anodic charge and OCP